IOP Publishing Journal of Physics: Condensed Matter
J. Phys.: Condens. Matter **27** (2015) 064113 (8pp) doi:10.1088/0953-8984/27/6/064113

Forced unraveling of chromatin fibers with nonuniform linker DNA lengths

Gungor Ozer[1], **Rosana Collepardo-Guevara**[2] **and Tamar Schlick**[1,3,4]

[1] Department of Chemistry, New York University, 100 Washington Square East, New York, NY 10003, USA
[2] Department of Chemistry, University of Cambridge, Cambridge CB2 1EW, UK
[3] Courant Institute of Mathematical Sciences, New York University, 251 Mercer Street, New York, NY 10012, USA
[4] NYU-ECNU Center for Computational Chemistry at NYU Shanghai, Shanghai 200062, China

E-mail: schlick@nyu.edu

Received 1 September 2014, revised 9 October 2014
Accepted for publication 17 October 2014
Published 7 January 2015

Abstract

The chromatin fiber undergoes significant structural changes during the cell's life cycle to modulate DNA accessibility. Detailed mechanisms of such structural transformations of chromatin fibers as affected by various internal and external conditions such as the ionic conditions of the medium, the linker DNA length, and the presence of linker histones, constitute an open challenge. Here we utilize Monte Carlo (MC) simulations of a coarse grained model of chromatin with nonuniform linker DNA lengths as found *in vivo* to help explain some aspects of this challenge. We investigate the unfolding mechanisms of chromatin fibers with alternating linker lengths of 26–62 bp and 44–79 bp using a series of end-to-end stretching trajectories with and without linker histones and compare results to uniform-linker-length fibers. We find that linker histones increase overall resistance of nonuniform fibers and lead to fiber unfolding with superbeads-on-a-string cluster transitions. Chromatin fibers with nonuniform linker DNA lengths display a more complex, multi-step yet smoother process of unfolding compared to their uniform counterparts, likely due to the existence of a more continuous range of nucleosome-nucleosome interactions. This finding echoes the theme that some heterogeneity in fiber component is biologically advantageous.

Keywords: chromatin, coarse-grained modeling, nonuniform NRL, alternating linker DNA length, Monte Carlo, force pulling

(Some figures may appear in colour only in the online journal)

1. Introduction

The genetic material of eukaryotic cells is stored in the nuclei in a highly condensed nucleoprotein complex where double-stranded DNA interacts with both core histone (two copies each of H2A, H2B, H3, H4) and linker histone (like H1 or H5) proteins. About 145–147 base pairs (bp) of DNA are wrapped around a protein octamer—consisting of two copies of each core histone—making ∼1.7 turns to form the nucleosome. Multiple nucleosomes are connected together by linker DNAs to define the chromatin fiber. With the addition of linker histones and under physiological salt conditions, the chromatin fiber can adopt an ordered state, long termed the 30 nm fiber [1]. Today, the existence of the 30 nm fiber *in vivo* has also come into question [2], with alternative proposals for a likely more abundant interdigitated state of 10 nm forms [3, 4]. Nonetheless, even the 30 nm wide fiber comes in multiple structural variations [5–7] and is likely polymorphic and dependent on many external and internal factors [8, 9]. Many higher-order states of packaging are recognized for interphase and metaphase chromosomes, but their details remain obscure [10].

Although the stability and condensed state of chromatin may be favored for long-term storage as well as genetic integrity, less ordered and more dynamic states are required to facilitate the biological activity and to make

 © 2015 IOP Publishing Ltd Printed in the UK

the genetic data accessible to molecular motors and other template-directed processes. Overall, understanding the folding/unfolding dynamics of chromatin fibers, and associated transitions between them, is of fundamental biological importance.

Various factors affect the folding of chromatin fibers, including the salt condition of the medium and the presence of linker histones (LHs) [11]. For instance, at low salt concentrations of <1 mM $MgCl_2$ and <100 mM NaCl, electrostatic repulsion between DNA segments is dominant and favors an extended fiber conformation called 'beads-on-a-string' [12, 13]. At physiological conditions of 150 mM NaCl and/or 2 mM $MgCl_2$, interfiber nucleosomal interactions counteract DNA–DNA repulsion, and the fiber can fold into a heteromorphic zigzag-like conformation (with a small percentage of bent linkers) of width 30 nm [14]. The importance of the LHs is that, by binding to the linker DNAs at the entry/exit point, they lead to stems which help stabilize compact conformations observed *in vivo* [15, 16], *in vitro* [17, 18], and *in silico* [11, 19].

Another variable that describes the compactness and spatial properties, and hence biological function, of chromatin fibers is the length of linker DNAs between nucleosomes. The length of the linker DNA plus the 145–147 bp of DNA wrapped around the histone core is often measured as a single parameter, the nucleosome repeat length (NRL). The average NRL can vary within the cell cycle and has been shown to be a significant factor of chromatin structure and function. For instance, electron microscopy (EM) and x-ray scattering studies [20–22] of various nuclosomal arrays revealed that a short (167 bp) NRL leads to fibers that are thin (21 nm) and less compact (6 nucleosomes per 11 nm), whereas medium (177–207 bp) NRLs lead to 34 nm fibers with 11 nucleosomes per 11 nm; long (217–247 bp) NRLs form fibers of 43 nm diameter and 15 nucleosomes per 11 nm packing density [23]. Similar results are obtained from all-atom [24] and coarse-grained computational studies [25, 26]. Our mesoscale chromatin model further reported narrow ladder-like chromatin fiber with short (182 bp) NRL, compact zigzag fibers with medium (191 and 209 bp) NRL, and heteromorphic fibers with long (218 and 226 bp) NRL [7, 8, 27, 28].

The studies above provide significant information about the structure of chromatin with various NRLs. However, in the cellular environment, other biomolecules and agents are present, and the NRL itself is nonuniform within a single fiber [29]. Although small alterations of the linker DNA length (2–4 bp) may have little effect on chromatin folding [30, 31], large deviations (>10 bp) could lead to changes in the overall structure of chromatin. For example, a 9-nucleosome chromatin fiber of extrachromosomal yeast consisting of 1453 bp with a very short NRL (∼160 bp) forms a circle-like structure [32]. Chromatin loops are formed between the two silencers of an HMRa locus which consists of 12 nucleosome with alternating NRL (152 bp and 167 bp) [33].

Recently, Collepardo-Guevara and Schlick reported highly polymporphic stable conformations of chromatin fibers with nonuniform NRL, grouped into three major categories depending on the NRL difference: canonical zigzag, bent ladder, and polymorphic [9]. They found not only that NRL variations introduce a large amount of polymorphism including loops and highly-curved forms that are stabilized by long-range internucleosome interactions, but also that fibers with a modest degree of linker-length variation can be more compact than fibers with uniform NRL. This suggests an important regulatory role for linker DNA length on chromatin structure and possibly function. Indeed, because the biological function of chromatin depends on the instantaneous form that the fiber adopts, it is essential to investigate the unfolding mechanisms of nonuniform linker-length chromatin fibers under external tension, as relevant to molecular motors.

Here we investigate the unfolding of two 24-nucleosome chromatin systems with alternating 173–209 bp NRL (26–62 bp linker DNA) and 191–226 bp NRL (44–79 bp linker DNA). Collepardo-Guevara and Schlick have shown that chromatin fibers with a 173–209 bp alternating NRL display compaction characteristics of a uniform 173 bp fiber [9], which makes the 173–209 bp fiber an interesting system to investigate. Similarly, a 191–226 bp alternating NRL fiber is also interesting, as it has greater compaction than the uniform counterpart, 209 bp NRL [9]. We apply forces up to 50 pN to stretch the fibers and generate force-extension curves. We compare the results to analogous 24-nucleosome systems with uniform NRL of various lengths obtained from computational and experimental studies. Available for reference are computed force-extension curves of uniform 173 bp and 209 bp fibers [34] with and without linker histones [19].

Not surprisingly, the addition of the linker histones increases the stiffness in our alternating NRL fibers as well. However, we observe a multi-step unfolding mechanism not present in the uniform NRL curves. This smoother behavior stems from the existence of a more continuous range of internucleosome contacts.

2. Materials and methods

2.1. Mesoscopic model of chromatin fiber

Our chromatin model [35–37] (figure 1(A)) treats the chromatin fiber as a combination of nucleosomes linked together with worm-like-chain beads of DNA. The nucleosome core with its wrapped DNA is modeled as an irregularly shaped rigid body of uniformly distributed 300 Debye–Hückel charges. The charges on the nucleosome are placed directly on the surface and interact with other nucleosomes, linker DNAs, and histone tails. Each linker DNA bead represents 9 base pairs with an equilibrium size of 3 nm. The systems studied in this work, fibers with alternating 26–62 and 44–79 bp linker DNA length, are represented with alternating 2–6 and 4–8 beads of linker DNA, respectively [7]. N-terminal tails of all four core histones and the C-terminal tail of H2A are explicitly modeled as coarse grained protein beads using the united-atom protein model [38] so that every 5 amino acids define a bead. Linker histones are modeled more coarsely where the relatively uncharged N-tail is neglected and three beads represent the long 111 amino-acid C-tail domain. The total

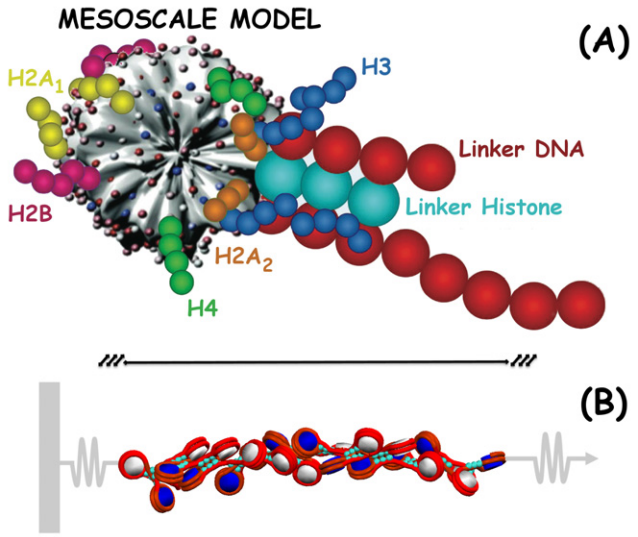

Figure 1. Chromatin model and fiber pulling setup. (A) The basic building block of our mesoscale chromatin model is displayed on a single nucleosome with a linker histone and alternating 44–79 bp linker DNA (corresponding to 4–8 beads in our coarse-grained resolution). The nucleosome core plus the wrapped DNA is modeled as uniformly distributed charges. Core histone tails, linker histones and linker DNAs are modeled explicitly as coarse-grained beads. (B) The pulling procedure for a fiber is illustrated.

potential energy of an oligonucleosome chain in our model consists of twisting, stretching, and bending terms of the linker DNAs; stretching and bending terms of the tails and linker histones; and total electrostatics and excluded volume terms. Monte Carlo sampling is implemented as pivot, translational, and rotational moves of the linker DNAs and nucleosome cores; tail regrowth; and linker histone reorganization. A detailed description of the energy parameters and MC moves can be found in [35–37].

2.2. Simulation details and fibers studied

We investigate two chromatin systems with alternating linker DNA lengths, 173–209 and 191–226 bp NRL, in a series of force induced Monte Carlo (MC) simulations at 293 K in a salt buffer of 150 mM of NaCl. The systems studied represent the 'bent-ladder' and 'polymorphic' architectures of nonuniform chromatin fibers [9]. The nonuniform bent-ladder structure of 173–209 bp fiber shows similar compaction characteristics as the uniform 173 bp fiber under zero mechanical stress. Chromatin fibers with longer nonuniform NRL, on the other hand, are quite different than their uniform counterpart with (+LH) and without (−LH) linker histones.

Here we confirm the above mentioned characteristic difference between nonuniform and uniform fibers in terms of corresponding internucleosomal interaction patterns. We define nucleosomes i and j to be in contact if the core charges or core-histone tails of nucleosome i is within 1.8 nm of the core charges or core-histone tails of nucleosome j [37], and generate the nucleosome–nucleosome contact map throughout the MC trajectory. We then calculate the normalized occurrence probability of each $i \pm k$ contact and obtain the corresponding ensemble averages. Figure 2 shows the equilibrium distribution for the zero pulling force. With LH, for instance, the nonuniform 191–226 bp fiber is polymorphic with dominant nucleosome–nucleosome interactions of $i \rightarrow i \pm 2, 3, 5$ and some longer-range interactions. Its uniform analogue, the 209 bp fiber, is more ordered ('canonical zigzag'), mostly making $i \rightarrow i \pm 2, 5$ contacts with LH and containing more higher-order interactions without LH.

For zero and all other pulling forces, we examine both nonuniform systems in the presence and absence of LHs. The initial coordinates of both systems are taken from [9]. To eliminate interference from other factors, all degrees of freedom (salt concentration, LH per nucleosome ratio, etc) are the same as in the nonuniform NRL [9] and uniform NRL pulling [11, 34] studies.

We apply a range of forces on each system and calculate the end-to-end displacement as a function of the applied force. To obtain a reliable description of the force-extension curves, we use different magnitudes of forces depending on the system. For example, the fibers are easier to unfold in the absence of linker histones ('−LH' in our notation), so less force is needed to cause larger extensions compared to the LH case. Similarly, fibers with shorter linkers are more resistant to unfolding and thus require greater forces to reach the same extension compared to longer linkers.

For every simulation set, we generate 9 trajectories at the mean DNA twist angle, and at $\pm 12^\circ$ DNA twist deviations from the mean, via 3 trajectories per twist angle. Each trajectory consists of up to 75 million MC steps; convergence is well achieved within 60 million steps. For a statistically meaningful analysis, we consider the last 10 million steps. The data shown here represent averages calculated from the coordinate trajectories recorded every 100 000 steps except for the end-to-end distance and energetics of the fiber which are recorded every 10 000 steps.

2.3. Stretching the chromatin fiber

Fiber stretching is implemented by fixing the first nucleosome to its initial coordinate and pulling the last nucleosome through the use of constant force along the Z-direction of the end-to-end vector of the fiber (figure 1(B)). In this protocol, the energy function of the system is modified with a potential directly proportional to the negative of the applied biasing force. The total energy of the system becomes:

$$E_{\mathrm{TOT}} = E_{\mathrm{TOT}} - F_{\mathrm{Pull}}|\vec{R}|, \tag{1}$$

where F_{Pull} is the added force, and $|\vec{R}|$ is the order parameter, namely the modulus of the end-to-end vector in the Z-direction, $|\vec{R}_{N,z} - \vec{R}_{1,z}|$, between the two terminal nucleosomes of the chromatin fiber. Depending on the magnitude of the pulling force, equation (1) translates into sampling the equilibrated system at force-induced extensions. The whole range of extension is sampled by repeated force pulling at specific forces. This Monte Carlo procedure is not intended to study time dependence. In terms of the central results (i.e. force extension dependence), our protocol resembles closely experimental single molecule perturbation techniques such

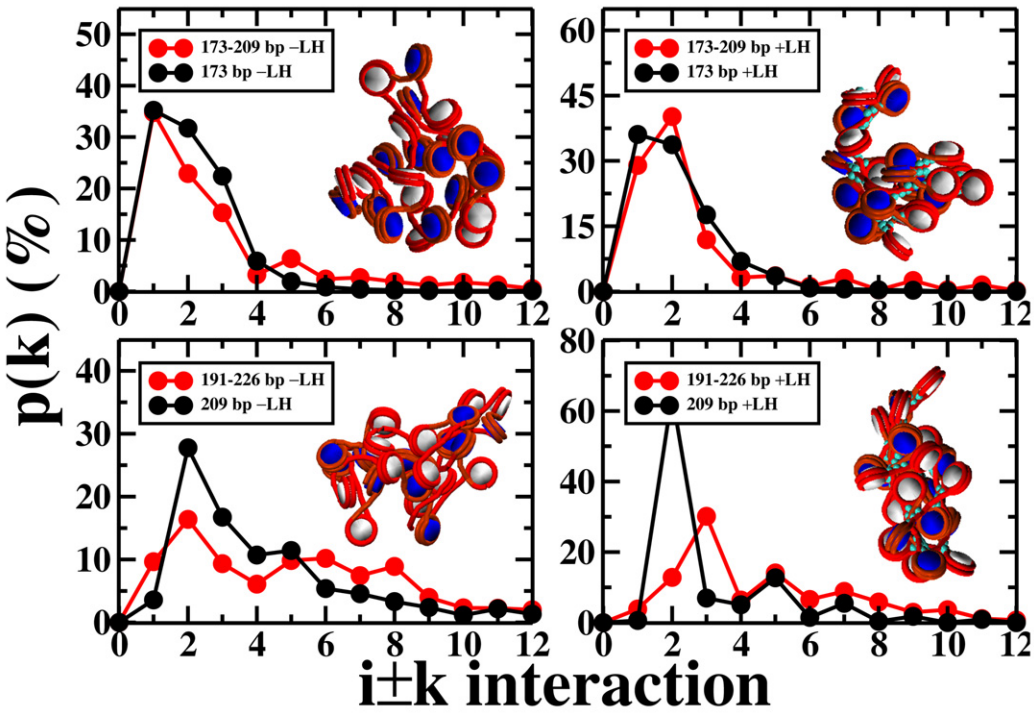

Figure 2. Probability distributions of the $i \pm k$ nucleosome-nucleosome interactions for equilibrium fiber confirmations at different conditions. Top panels represent data for alternating 173–209 bp and uniform 173 bp fibers; bottom panels correspond to alternating 191–226 bp NRL and uniform 209 bp fibers, respectively. The nonuniform 173–209 bp fiber is a 'bent-ladder' with dominant $i \rightarrow i \pm 1, 2, 3$ internucleosome interactions. The 191–226 fiber adopts a polymorphic structure with $i \rightarrow i \pm 2, 3, 5$ contacts, different than its uniform counterpart, 209 bp fiber. The left and right panels correspond to models without linker histones and with linker histones, respectively.

as atomic force microscopy (AFM). In fact, constant force pulling can be considered as atomic force microscopy *in silico*. Therefore, the results from such computational studies can complement experimental findings [19, 25, 39–42].

3. Results

Figures 3 and 4 present the resulting force-extension curves and snapshots for nonuniform and uniform fibers without and with linker histones, respectively. Figure 5 compares behavior with, versus without, linker histones, and figure 6 provides internucleosome contacts for equilibrium fibers at different values of applied force.

3.1. Longer linker DNAs soften the nonuniform fiber response to stretching forces in the absence of linker histones

Without linker histones, chromatin fibers with nonuniform linker DNA lengths display a softer response to the pulling force and unfold more smoothly. Similar smooth unfolding mechanisms are reported in previous force-stretching experiments [11, 19] with uniform NRL fibers. This behaviour may be attributed to rapid exchange between the compact and fully stretched chromatin configurations in organisms with short life spans and high reproduction rates [43].

Figure 3 shows that the 191–226 bp fiber unfolds with little resistance at the low force regime. It extends from the initially compact conformation (46 nm) to a largely unfolded conformation (361 nm) with 6 pN of applied force. Figure 6 indicates that almost all of the internucleosome interactions within the 191–226 bp fiber are $i \rightarrow i \pm 1$ by 6 pN. By 10.5 pN, the fiber extends to 468 nm and loses all nucleosome–nucleosome interactions very rarely forming $i \rightarrow i \pm 1$ contacts. At that point, the fiber becomes more resistant to stretching and accommodates only 225 nm of additional unfolding up to 30 pN.

The 173–209 bp fiber is more resistant to stretching, especially at low forces (2–8 pN) and extremely high forces (20–40 pN). The 173–209 bp fiber unfolds only partially to 219 nm by 8 pN, followed by a faster unfolding up to 470 nm at the medium force regime (10–20 pN). At this medium force regime, the fiber has already lost most of the nonbonded internucleosome contacts and establishes only $i \rightarrow i \pm 1$ interactions. Beyond 20 pN, it becomes extremely resistant, accommodating, for instance, a mere 47 nm of additional stretch between 30 pN and 40 pN. The overall softening of the fiber stiffness with increasing NRL is also visible between the nonuniform 173–209 fiber (average NRL 191 bp) and uniform 173 bp fiber.

3.2. Linker histones increase nonuniform fiber's overall resistance to unfolding, and lead to more complex unfolding patterns

When LHs are placed in contact with the linker DNAs at the entry/exit point, they stabilize the DNA stems by immobilizing the entering/exiting linker DNAs [19, 44]. As a result,

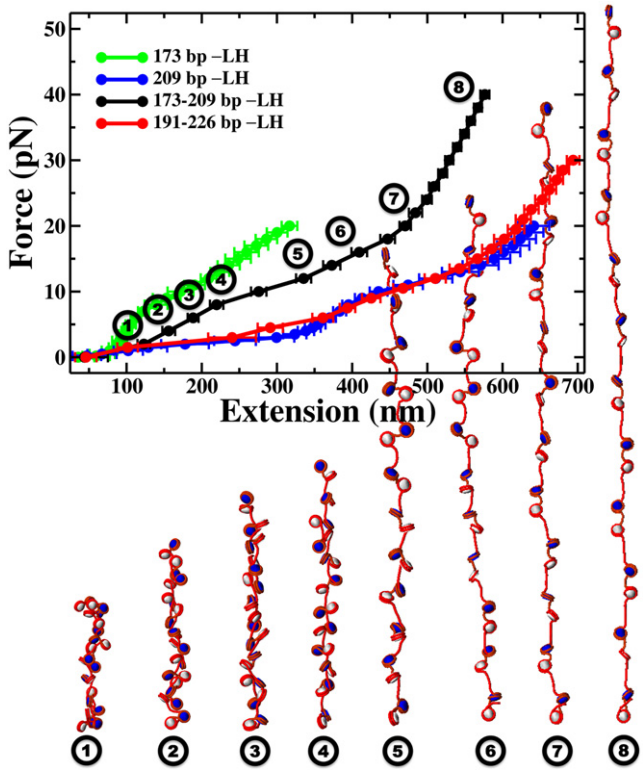

Figure 3. Stretching response of chromatin fibers with alternating versus uniform linker DNA length in the absence of linker histones (−LH). Black and red curves represent the force-extension data for alternating 173–209 bp and 191–226 bp NRL fibers; green and blue curves represent the same data for the uniform 173 bp and 209 bp fibers, respectively. Error bars denote standard deviations from the mean end-to-end separation of each force-specific ensemble. The snapshots represent the minimum energy configuration selected from the equilibrium ensemble of the chromatin fiber stretched using the labeled (circled) forces. The forces corresponding to snapshots 1–8 are 2, 4, 6, 8, 12, 16, 22 and 40 pN, respectively.

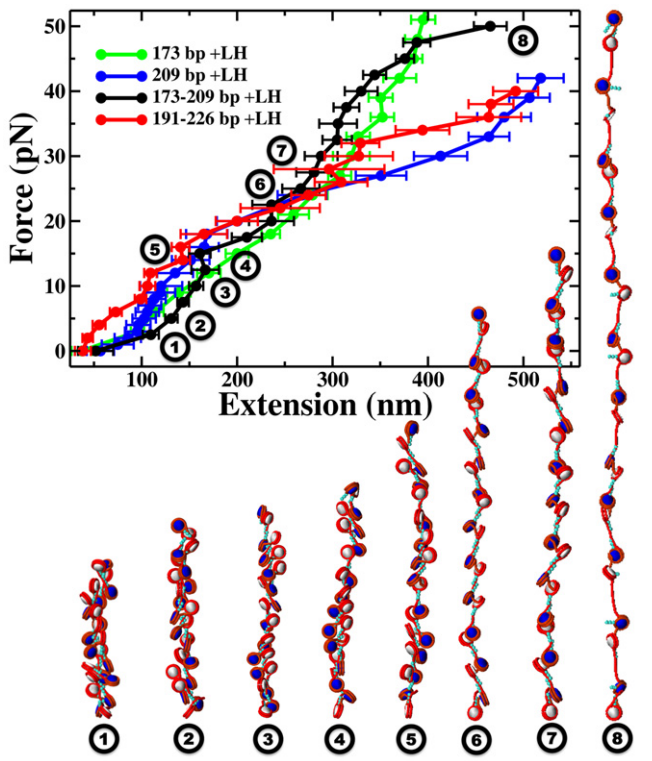

Figure 4. Stretching response of chromatin fibers with alternating versus uniform linker DNA length in the presence of linker histones (+LH). Black and red curves represent the force-extension data for alternating 173–209 bp and 191–226 bp NRL fibers; green and blue curves represent the same data for the uniform 173 bp and 209 bp fibers, respectively. Error bars denote standard deviations from the mean end-to-end separation of each force-specific ensemble. The snapshots represent the minimum energy configuration selected from the equilibrium ensemble of the chromatin fiber stretched using the labeled (circled) forces. The forces corresponding to snapshots 1–8 are 2.5, 5, 10, 12.5, 15, 25, 30 and 50 pN, respectively.

chromatin fibers adopt more compact structures compared to those without LHs. In force pulling simulations, this translates into greater resistance to fiber stretching. The higher resistance to unfolding due to the addition of linker histones had previously been observed for uniform NRL fibers [11, 19]. Not surprisingly, we see the same effect for both our nonuniform NRL fibers in figure 4.

For the 173–209 bp NRL fiber, without LHs, even at low forces (<10 pN) the fiber extends to ∼350 nm (figure 3). With LHs, the same extension requires extremely large force (∼45 pN). Nonbonded internucleosomal interactions are all broken by 10 pN without LHs, but >20 pN forces are required with LHs. We observe similar behavior for the 191–226 fiber. Without LH, the fiber unfolds to 425 nm extension with only 10 pN of applied force compared to 35 pN in the presence of linker histones. We see a remarkable difference in our internucleosomal interactions analysis for the nonuniform 191–226 fiber. By 6 pN, the $i \pm 1$ contacts become dominant in the case of −LH. With LHs, this does not happen until 34 pN where we still observe considerable amount of $i \pm 2$ and $i \pm 3$ contacts.

Interestingly, figure 4 shows that the fiber softening pattern as the linker DNA length increases is reversed at the low force regime. The shorter 173–209 fiber unfolds to larger extensions at low/medium force regime compared to the long 191–226 fiber. At higher forces (>20 pN), the 191–226 fiber extends further. This behavior had previously been observed for uniform fibers [19] in which the 209 bp fiber displays stiffer characteristics at medium force regime compared to 173 bp fiber.

Linker histones introduce a more complex multi-step unfolding mechanism due to the formation of DNA stems which reorganize the chromatin fiber. The irregular pattern of the force-extension curve with linker histones is caused by the energetic barriers needed to be overcome breaking DNA stems as well as the irregular 'superbeads', involving clusters of nucleosomes. Figure 6 shows that, for the 173–209 bp fiber, $i \pm 2$ contacts are gradually replaced by $i \pm 1$ contacts as the applied force increases from 0 pN to 15 pN; interestingly, the $i \pm 3$ contacts are preserved throughout this transformation. This is only possible when small clusters of energetically stable nucleosomes remain together during unfolding. After the 173–209 bp fiber straightens (by 15 pN), the clusters begin to separate, and by 20 pN all nonbonded internuclosomal interactions are deformed This is visible in the explicit snapshots in figure 4.

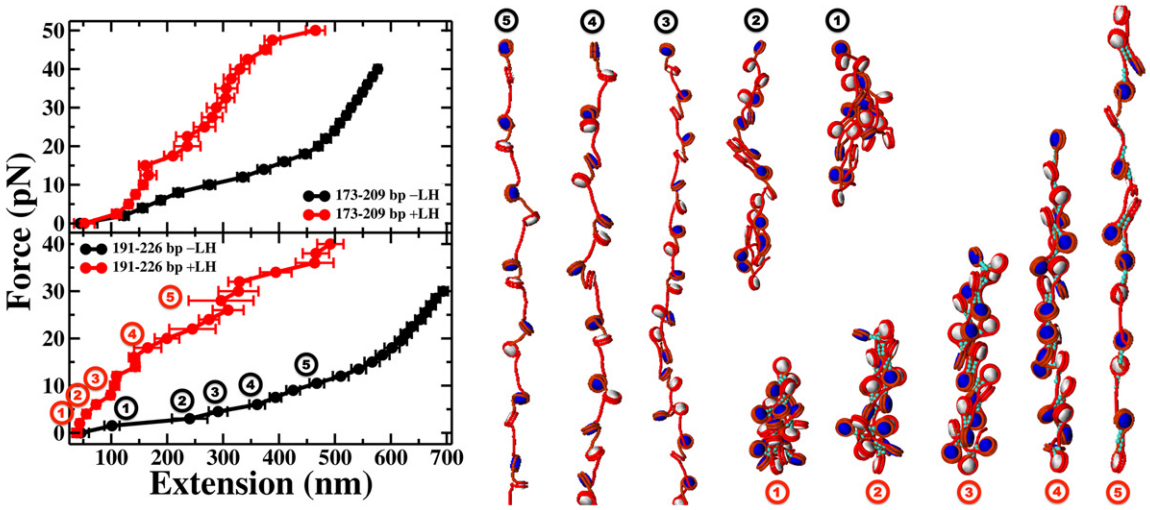

Figure 5. Stretching response of chromatin fibers with alternating linker DNA lengths in the presence (red) and absence (black) of linker histones. Top and bottom panels represent data for 173–209 bp and 191–226 bp NRL fibers, respectively. Error bars denote standard deviations from the mean end-to-end separation of each force-specific ensemble. The snapshots (in black tags without LH and red with LH) correspond to minimum energy configuration selected from the equilibrium ensemble of the chromatin fiber with alternating 44–79 bp linker DNA length (or 191–226 bp in NRL units) stretched using the labeled (circled numbers) forces. The forces correspond to snapshots 1–5 are 1.5, 3, 4.5, 6 and 10.5 pN for the −LH case; 2, 4, 8, 20 and 30 pN for the +LH case (red), respectively.

Similarly, for the 191–226 bp fiber, the complex force-extension curve can be attributed to formation and rupture of nucleosome clusters of various shape. The initial conformation of 191–226 bp fiber is more compact with the presence of longer-range contacts (i.e., $i \rightarrow i \pm 6$ or longer). During the initial fiber straightening (0–12 pN), these long-range interactions are replaced by $i \pm 2, 3, 5$ interactions to form stable clusters (figure 6). These clusters then start to rupture as the applied force increases to 20 pN. Still, even at 34 pN of stretching force, small clusters formed between i and $i \pm 2$ and $i \pm 3$ nucleosomes exist.

3.3. The effect of linker histones becomes more pronounced as the nonuniform linker DNA length increases

By comparing figures 3 and 4, we see that both nonuniform fibers become more resistant to stretching with LH. The extent of the added stiffness, however, depends on the length of the linker DNA. In the top panel of figure 5 we see that the two curves for the 173–209 bp fiber with and without LHs initially overlap but start diverging after a 150 nm end-to-end separation. In contrast, the two systems begin to diverge at shorter separation for the 191–226 bp NRL fiber (figure 5, bottom). This is expected because, without linker histones, the major contribution to overall fiber compaction comes from the non-parental core histone tail interactions, which cannot absorb mechanical stretching. When LHs are inserted, the entering/exiting DNAs become more rigid, and this contributes to the overall fiber compaction and increased resistance to unfolding. This contribution by LHs is larger for fibers with longer linker DNA lengths which contain irregular long-range nucleosome-nucleosome interactions [22].

3.4. Fibers with nonuniform NRL exhibit different unfolding mechanisms compared to their uniform counterparts

The 191–226 bp fiber has 62 base pairs of linker DNA on average. The range of the fiber extension, therefore, is identical to that of a chromatin fiber with 62 bp uniform linker length (209 bp NRL). Although the force-extension curves are also similar, the transition is somewhat smoother in the nonuniform case both in the presence and absence of LHs. Without LH, Collepardo-Guevara and Schlick observed a distinctive structural transition around 350–400 nm stretching of the uniform NRL fiber [11, 34] which is not as pronounced in the nonuniform NRL fiber shown in figure 3. When LHs are introduced, both nonuniform and uniform NRL fibers become more resistant to stretching (figure 4). However, the uniform fiber displays less progressive transition states compared to the nonuniform fiber. We see in figure 6 that the nonuniform 191–226 bp fiber with LH undergoes a multi-step unfolding process, which involves transformation of long-range contacts first to $i \pm 2, 3, 5$ (characteristics of a canonical zigzag fiber with 5 nucleosomes per turn) up to 20 pN, and then a gradual transformation to $i \pm 1$ (single stack of nucleosomes) by 40 pN. This suggests that long-range interactions are weaker and lost initially during the unfolding of polymorphic chromatin fibers.

Similarly, although the structural properties of the 173 bp uniform NRL fiber and the 173–209 bp nonuniform fiber are similar (see figure 2), their unfolding mechanisms differ. Figure 4 shows that the force-extension diagram of the alternating 173–209 bp fiber is continuously shifted to greater extension. When linker histones are added, the difference at the low force regime is smaller, and the trend reverses for medium forces where the uniform 173 bp fiber is slightly longer than the nonuniform 173–209 bp fiber. This behavior is likely due to disruption of unbalanced stem formation in these fibers.

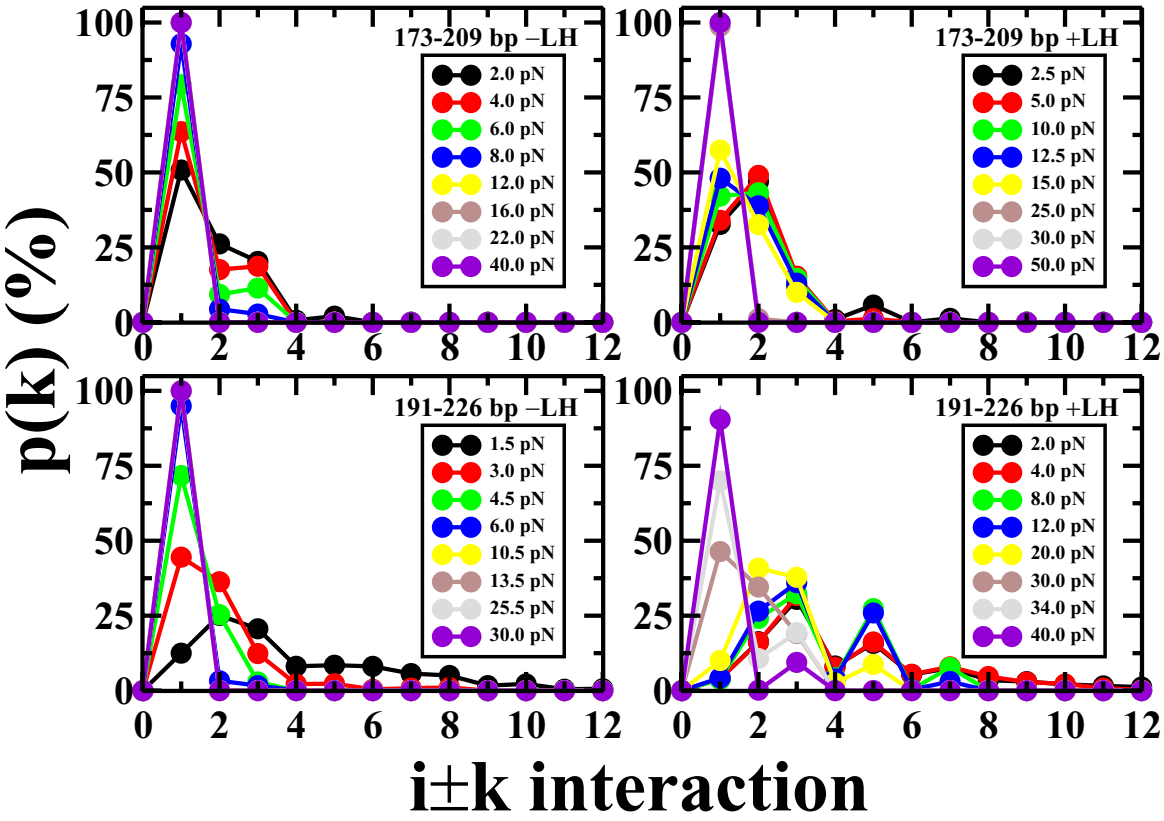

Figure 6. Probability distributions of the $i \pm k$ nucleosome–nucleosome interactions for equilibrium fibers at different applied forces. Top panels represent data for the alternating 173–209 bp fiber, and bottom panels correspond to the alternating 191–226 bp NRL fiber. The left and right panels correspond to models without histones and with linker histones, respectively.

4. Discussion

The architecture and dynamics of chromatin fibers depend on various factors such as the number of nucleosomes, linker DNA length, the presence/absence of linker histones (LH), the monovalent and divalent salt concentration of the medium, and many more factors. Significant effort has been devoted to model such aspects of chromatin fibers *in silico*. Much of the computational research regarding chromatin structure and function assumes homogenous linker DNA length. However, the linker DNA length within the cell or even within a single chromatin fiber may be heterogenous *in vivo*. To obtain a more representative view of the *in vivo* characteristics of chromatin fibers, the heterogenous nature of the NRL should also be considered *in silico*. In this context, we take the alternating distribution of linker lengths into account in our mesoscale model and implement force induced unfolding simulations.

The average NRL values for our nonuniform 173–209 bp and 191–226 bp fibers, namely 191 (linker DNA length of 44 bp) and 209 (linker DNA length of 62 bp), occur for the most abundant fibers found in nature [45, 46] with linker histone H1. The observed compaction with H1 [16, 18, 44] translates into stiffer fiber response to mechanical stretching in single molecule manipulation studies [11, 19, 42].

We find that the inhomogenous linker-length fibers with LH display different unfolding characteristics compared to their uniform NRL counterparts. Specifically, we find that the unfolding of nonuniform chromatin fibers in the presence of linker histones is a multi-step process which results in more complex yet smoother force-extension curves in the force stretching simulations. This smoother, more progressive series of structural jumps can be explained by the larger and more continuous range of internucleosome contacts present in the nonuniform fibers (figures 4 and 6).

Indeed, such clumps of nucleosomes, or 'superbeads', have been observed in various cell types [47] and in our prior work [9]. A more recent AFM study revealed that the size of such fragments can be experimentally modulated by varying the monovalent and divalent salt concentration [46]. Here we suggest that the formation, stability, and rupture of superbeads can also be modulated by nonuniformly altering the linker-DNA lengths, which further affects the unfolding mechanism of chromatin fibers. Our finding that some degree of heterogeneity can lead to smoother unfolding resembles the message that heterogenous chromatin fibers with small differences in linker lengths can produce more compact fibers than uniform linker analogues [9].

In real chromatin fibers, unwrapping of nucleosomes is likely to occur at high force regime with LH or even at lower force regime without LH [41]. Laser and optical tweezer experiments reveal that nucleosome disassembly may occur at 20–40 pN [48, 49]. Recent histone posttranslational modifications (PTMs) studies also show that modifications affecting the DNA entry-exit region induce/inhibit transient nucleosome disassembly [50]. Natural extensions of our work

involve a systematic modeling of such nucleosome unwrapping effects.

Acknowledgments

Computing support from the New York University High Performance Computing Mercer cluster and Blue Gene at CCNI (RPI) is acknowledged. This work was supported by the National Institutes of Health (R01 GM55164 to TS), Philip Morris USA and Philip Morris International (to TS). The authors thank Dr Antoni Luque for insightful discussions.

References

[1] Finch J and Klug A 2011 *Proc. Natl Acad. Sci. USA* **73** 1897
[2] Maeshima K, Hihara S and Eltsov M 2010 *Curr. Opin. Cell Biol.* **22** 291
[3] Eltsov M, MacLellan K M, Maeshima K, Frangakis A S and Dubochet J 2008 *Proc. Natl Acad. Sci. USA* **105** 19732
[4] McDowall A, Smith J and Dubochet J 1986 *EMBO J.* **5** 1395
[5] Woodcock C, Frado L and Rattner J 1984 *J. Cell Biol.* **99** 42
[6] van Holde K and Zlatanova J 2007 *Semin. Cell Dev. Biol.* **18** 651
[7] Perišić O, Collepardo-Guevara R and Schlick T 2010 *J. Mol. Biol.* **403** 777
[8] Grigoryev S, Arya G, Correll S, Woodcock C and Schlick T 2009 *Proc. Natl Acad. Sci. USA* **106** 13317
[9] Collepardo-Guevara R and Schlick T 2014 *Proc. Natl Acad. Sci. USA* **111** 8061–6
[10] Maeshima K, Imai R, Tamura S and Nozaki T 2014 *Chromosoma* **123** 225
[11] Collepardo-Guevara R and Schlick T 2012 *Nucl. Acids Res.* **40** 8803
[12] Olins A and Olins D E 1974 *Science* **183** 330
[13] Olins D E and Olins A 2003 *Nat. Rev. Mol. Cell Biol.* **4** 809
[14] Sun J, Zhang Q and Schlick T 2005 *Proc. Natl Acad. Sci. USA* **102** 8180
[15] Lever M, Th'ng J, Sun X and Hendzel M 2000 *Nature* **408** 873
[16] Misteli T, Gunjan A, Hock R, Bustin M and Brown D 2000 *Nature* **408** 877
[17] Caron F and Thomas J 1981 *J. Mol. Biol.* **146** 513
[18] Robinson P J, An W, Routh A, Martino F, Chapman L, Roeder R G and Rhodes D 2008 *J. Mol. Biol.* **381** 816
[19] Collepardo-Guevara R and Schlick T 2011 *Biophys. J.* **111** 1670
[20] Williams S, Athey B, Muglia L, Schappe R, Gough A and Langmore J 1986 *Biophys. J.* **49** 233
[21] Robinson P, Fairall L, Huynh V and Rhodes D 2006 *Proc. Natl Acad. Sci. USA* **103** 6506
[22] Routh A, Sandin S and Rhodes D 2008 *Proc. Natl Acad. Sci. USA* **105** 8872
[23] Szerlong H J and Hansen J C 2011 *Biochem. Cell Biol.* **89** 24
[24] Wong H, Victor J and Mozziconacci J 2007 *PLoS One* **2** e877
[25] Katritch V, Bustamante C and Olson W 2000 *J. Mol. Biol.* **295** 29
[26] Aumann F, Sühnel J, Langowski J and Diekmann S 2010 *Theor. Chem. Acc.* **125** 217
[27] Kruithof M, Chien F, Routh A, Rhodes C and van Noort J 2009 *Nat. Struct. Mol. Biol.* **16** 534
[28] Schlick T and Perišić O 2009 *Phys. Chem. Chem. Phys.* **1** 10729
[29] Prunell A and Kornberg R 1982 *J. Mol. Biol.* **154** 515
[30] Grigoryev S 2012 *Nucleus* **3** 493
[31] Correll S, Schubert M and Grigoryev S 2012 *EMBO J.* **31** 2416
[32] Thoma F, Bergman L and Simpson R 1984 *J. Mol. Biol.* **177** 715
[33] Ravindra A, Weiss K and Simpson R 1999 *Mol. Cell Biol.* **19** 7944
[34] Collepardo-Guevara R and Schlick T 2013 *Biochem. Soc. Trans.* **41** 494
[35] Beard D and Schlick T 2001 *Biopolymers* **58** 106
[36] Zhang Q, Beard D and Schlick T 2003 *J. Comput. Chem.* **24** 2063
[37] Sun J, Zhang Q and Schlick T 2006 *Biophys. J.* **91** 133
[38] Warshel A and Levitt M 1976 *J. Mol. Biol.* **103** 227
[39] Mergell B, Everaers R and Schiessel H 2004 *Phys. Rev.* E **70** 011915
[40] Aumann F, Lankas F, Caudron M and Langowski J 2006 *Phys. Rev.* E **73** 041927
[41] Kepper N, Ettig R, Stehr R, Marnach S, Wedemann G and Rippe K 2011 *Biopolymers* **95** 435
[42] Xiao B, Freedman B S, Miller K E, Heald R and Marko J F 2012 *Mol. Biol. Cell* **23** 4864
[43] Downs J A, Kosmidou E, Morgan A and Jackson S P 2003 *Mol. Cell* **11** 1685
[44] Bednar J, Horowitz R A, Grigoryev S A, Carruthers L M, Hansen J C, Koster A J and Woodcock C L 1998 *Proc. Natl Acad. Sci. USA* **95** 14173
[45] Widom J 1992 *Proc. Natl Acad. Sci. USA* **80** 1095
[46] Caño S, Caravaca J M, Martín M and Daban J-R 2006 *Eur. Biophys. J.* **35** 495
[47] Zentgraf H and Franke W W 1984 *J. Cell Biol.* **99** 272
[48] Cui Y and Bustamante C 2000 *Proc. Natl Acad. Sci. USA* **97** 127
[49] Bennink M L, Leuba S H, Leno G H, Zlatanova J, de Grooth B G and Greve J 2001 *Nat. Struct. Biol.* **8** 606
[50] Neumann H *et al* 2009 *Mol. Cell* **36** 153